

Coulomb Stress Analysis of the 21 February 2008

$M_w= 6.0$ Wells, Nevada, Earthquake

Volkan Sevilgen

U. S. Geological Survey, Menlo Park, CA, vsevilgen@usgs.gov, 1 (650) 329 4803

Abstract

Static Coulomb stress changes imparted by the February 21, 2008 Wells, Nevada earthquake are calculated, using an 8x6 km rectangular patch with a uniform-slip as a source fault. Stress changes are resolved on nearby active faults using their rake, dip, strike direction, and assuming a fault friction of 0.4. The largest (0.2 bars) stress increase imparted to surrounding major active faults occurs on an unnamed fault (Fault A) that may be the continuation of the ruptured fault. A 0.1-bar stress increase is calculated on Snake fault. Stress decreases are calculated on the northern parts of the Independence and Ruby faults by 0.5 bars. The Coulomb stress change is calculated on relocated aftershocks assuming that they have the same strike dip and rake, as the source fault. Under this assumption; 75% of the aftershocks receive a Coulomb stress increase.

Introduction

The $M_w= 6.0$ Wells, Nevada, earthquake struck in the middle of the East Humboldt Range, near the southern end of the Snake Mountains and Wood Hills (Figure 1A). The active faults in the study area, which are located in the Basin and Range regime, are assumed to have a dip about 60° and have normal slip. Fault A and the source fault dip to the east, and the rest of the faults dip to the west (Craig dePolo, 2008 personal communication). The Central and Northern Ruby fault are about 15,000 years old (USGS, 2006) and have a slip rate of 0.2-0.5 mm/year (dePolo, 1998). The Independence fault is about 130,000 years old (Frankel et al., 2002; USGS, 2006) and has a slip rate of 0.2-0.5 mm/year (dePolo, 1998).

Method

Coulomb 3 (Toda et al., 2007; Toda et al., 2005; Lin and Stein, 2004; Toda et al., 2007) is used to calculate the static Coulomb stress change (Figure 1B), shear stress change (Figure 3A) and normal stress change (Figure 3B) on active fault planes to understand the changes of earthquake hazard on the surrounding faults. Fault friction coefficient is assumed of 0.4 in an elastic halfspace.

I used the relocated aftershocks to infer the location and geometry of the source fault with a strike of 35° and a 55° E dip (Figure 2A-B). Based on the observed hole in the seismicity, an 8 x 6 km rectangular source fault is assumed between 4.5 and 9.5 km depths (Figure 2B). Using -83° rake from the USGS' focal mechanism, 0.76 m normal and 0.09 m left-lateral slip is calculated to produce $M_0 = 1.18 \times 10^{25}$ dyne cm, $M_w = 6.0$. Some 75% of the 870 aftershocks as of August 12, 2008, are brought closer to failure by the main rupture assuming they have the same strike, dip and rake as the mainshock (Figure 2A-B). A cluster of aftershocks on the corner of the assumed source plane (Figure 2A-B), received a stress change decrease, perhaps because the assumed fault plane and uniform slip model is too simple.

Results: Coulomb stress changes on active fault planes

Fault A, which strikes 8° and dips 50° to the east, has the largest Coulomb stress increase, with an average of 0.22 bars (Figure 1B), because of unclamping and a shear stress increase. This small fault is important because it might be the southern extension of the rupture plane. The southern portion of the Snake fault, which strikes 135° and dips 60° to the west, has a stress increase with an average 0.1 bars. The shallow portion of Central Ruby fault (225° -striking 60° west-dipping normal fault) has a negligible Coulomb stress increase (< 0.05 bars) (Figure 1B).

A large Coulomb stress decrease of 0.5 bars is calculated on the northern portion of the Independence fault, which is a 180°-striking and 60°-west-dipping normal fault (Figure 1B), largely because of fault clamping on deeper parts (Figure 3B) and shear stress decrease on shallow parts. The southern portion has a negligible stress increase (< 0.05 bars). The Northern Ruby fault also has a large stress decrease by 0.5 bars, which is likely to inhibit Coulomb failure on the 195°-striking and 60° west-dipping normal fault, both because of fault clamping (0.57 bars) and shear stress decrease (0.35 bars).

Conclusion

The greatest Coulomb stress effect imparted from Wells earthquake was to promote failure on the Fault A through a shear stress increase and unclamping. Modest promotion of failure is seen along the southern part of the Snake fault and shallow depths of the Central Ruby fault. The Coulomb stress decrease on the northern part of the Independence fault and the Northern Ruby fault inhibit Coulomb failure.

Further monitoring and micro seismicity should reveal whether the calculated stress increases are associated with seismicity rate increases, which if found would point to an increased earthquake hazard.

Acknowledgments

I thank Ross Stein and Jeanne Hardeback for reviews

References

U.S. Geological Survey and Nevada Bureau of Mines and Geology, 2006, Quaternary fault and fold database for the United States, accessed Jan 9, 2006, from USGS web site: <http://earthquake.usgs.gov/regional/qfaults/>.

Toda S., Stein R., Lin J., Sevilgen V., Coulomb 3.1 Software, <http://www.coulombstress.org>, 2007

dePolo C. M., A reconnaissance technique for estimating the slip rates of normal-slip faults in the Great Basin, and application to faults in Nevada, U.S.A., Ph.D. Thesis, University of Nevada, Reno (John Anderson, Dissertation Advisor), 1998

Toda, S., R. S. Stein, K. Richards-Dinger and S. Bozkurt (2005), Forecasting the evolution of seismicity in southern California: Animations built on earthquake stress transfer, *J. Geophys. Res.*, B05S16, doi:10.1029/2004JB003415.

Lin, J. and R.S. Stein (2004), Stress triggering in thrust and subduction earthquakes, and stress interaction between the southern San Andreas and nearby thrust and strike-slip faults, *J. Geophys. Res.*, 109, B02303, doi:10.1029/2003JB002607.

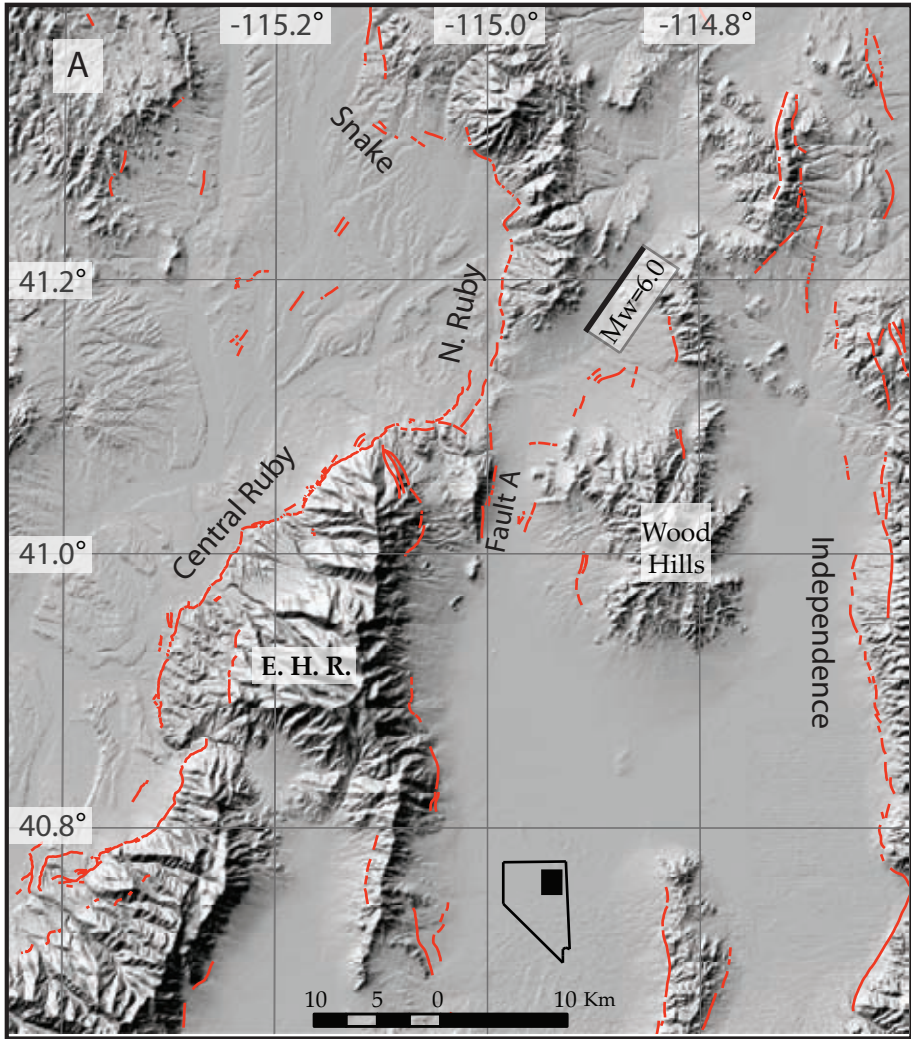
Figure captions:

Figure 1, A. Topography with active fault traces from quaternary fault database (REF). B. Coulomb Stress on modeled faults. Source fault has a 35°-strike, 55°NW dip, and -83° rake. Receiver faults: Fault A is 55°E-dipping Normal fault, and other receivers are 60° W-dipping Normal faults. Fault friction assumed 0.4.

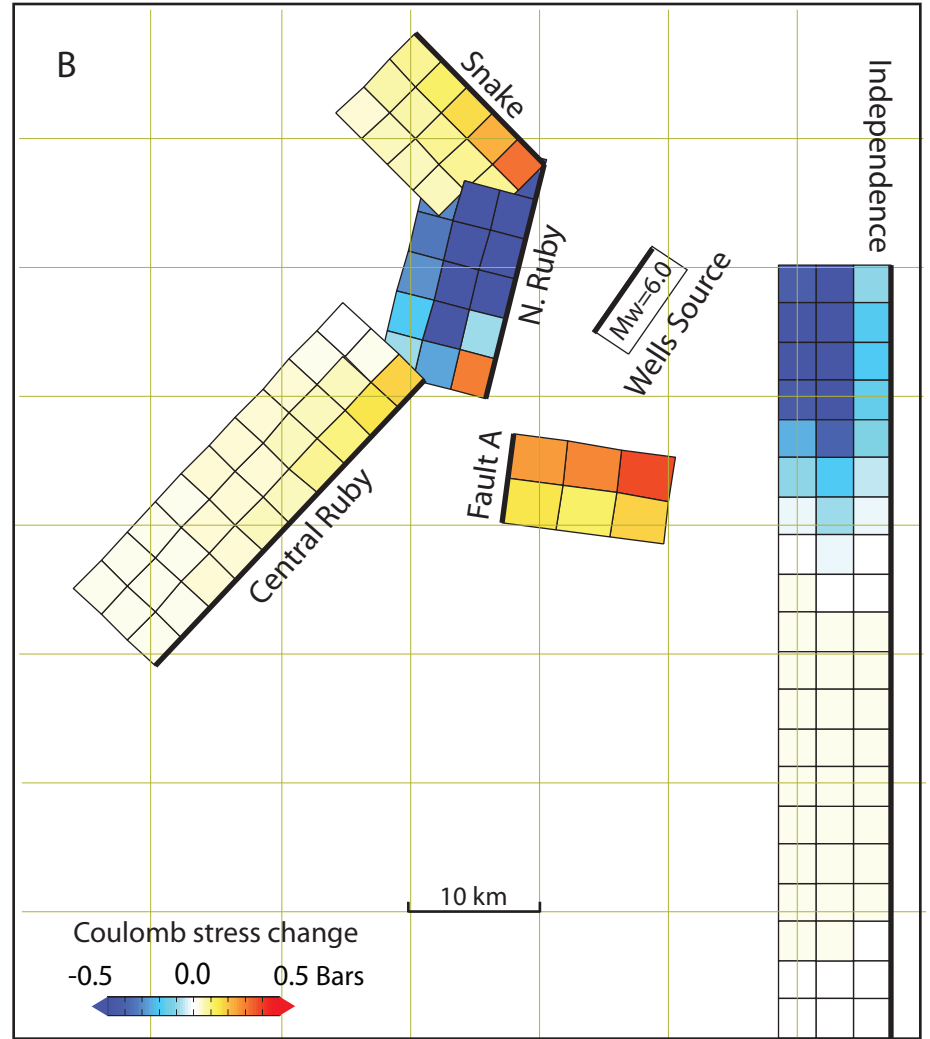
Figure 2, A. Coulomb stress change on aftershocks, assumed same strike, dip rake as mainshock. Friction coefficient is 0.4. B. Cross section.

Figure 3, A. Shear stress change on modeled faults. B. Normal stress change on modeled faults.

Active fault surface traces



Coulomb stresses on the modeled fault planes



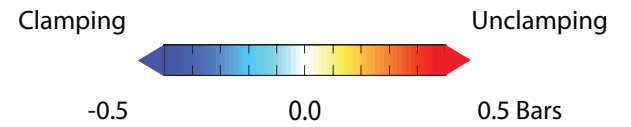
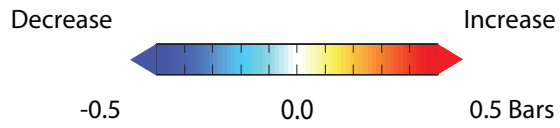
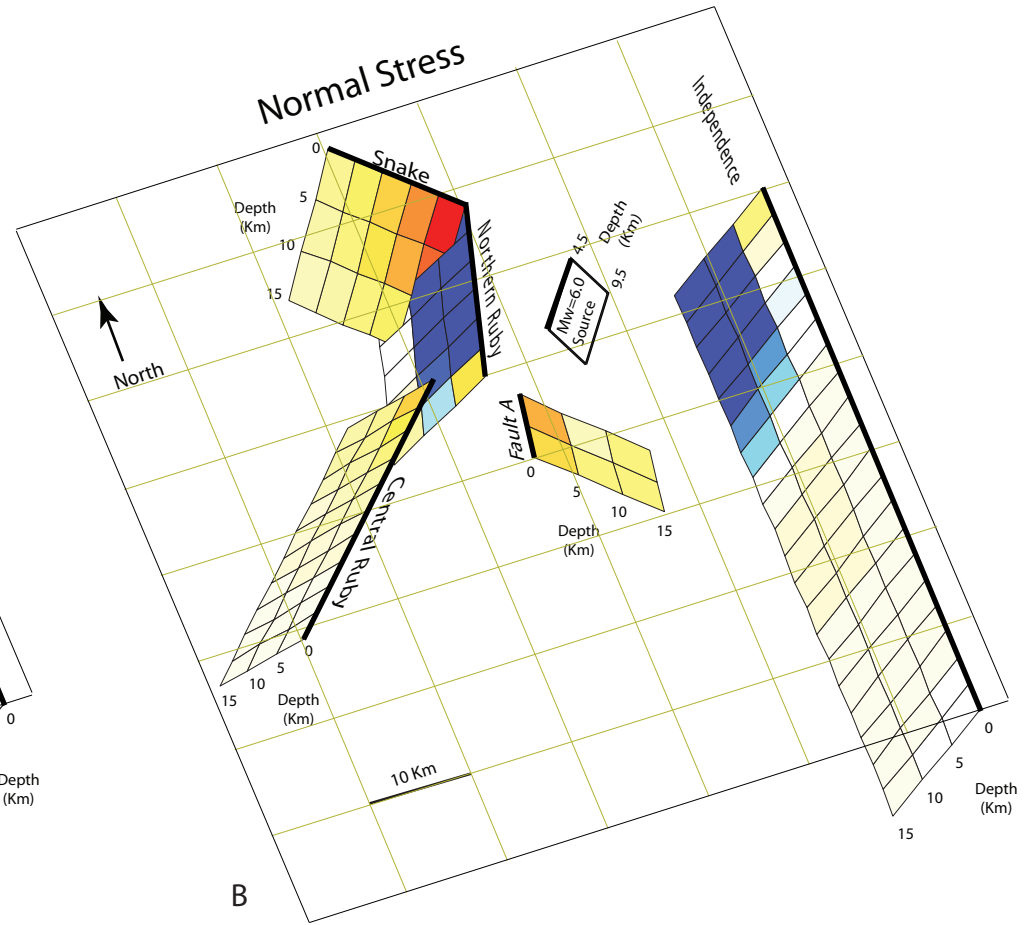
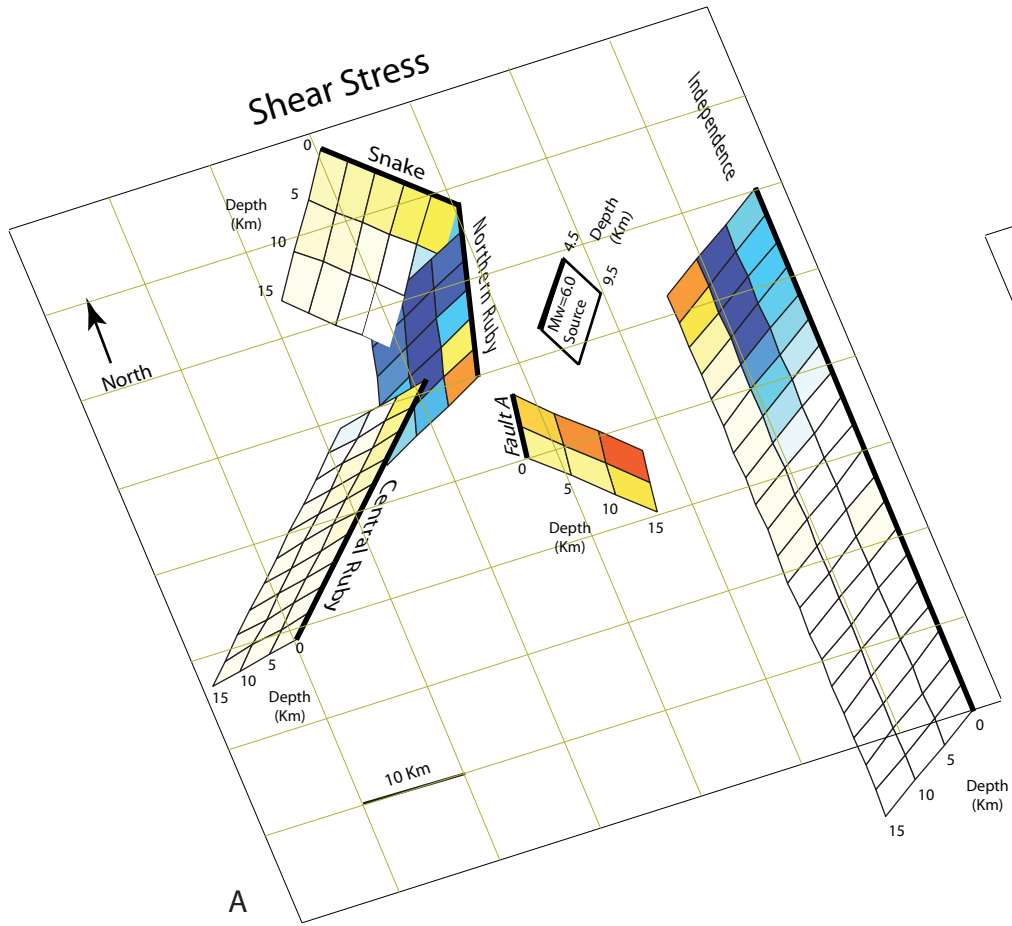


Figure 3
Sevilgen
01/23/2009